



**HAL**  
open science

## **Importance of PCDD/F molecules' polarizability and steric hindrance on their adsorption onto zeolites in a standard EN1948-1 sampling device for incinerator emission monitoring**

Oliver Schäf, Laurence Tortet, Angélique Simon-Masseron, Joël Patarin, Stephanie Defour, Rosine Blanc, Christophe Coste, Yves Zerega

### ► To cite this version:

Oliver Schäf, Laurence Tortet, Angélique Simon-Masseron, Joël Patarin, Stephanie Defour, et al.. Importance of PCDD/F molecules' polarizability and steric hindrance on their adsorption onto zeolites in a standard EN1948-1 sampling device for incinerator emission monitoring. *Chemosphere*, 2020, 259, pp.127457. 10.1016/j.chemosphere.2020.127457 . hal-02885557

**HAL Id: hal-02885557**

**<https://hal.science/hal-02885557>**

Submitted on 30 Jun 2020

**HAL** is a multi-disciplinary open access archive for the deposit and dissemination of scientific research documents, whether they are published or not. The documents may come from teaching and research institutions in France or abroad, or from public or private research centers.

L'archive ouverte pluridisciplinaire **HAL**, est destinée au dépôt et à la diffusion de documents scientifiques de niveau recherche, publiés ou non, émanant des établissements d'enseignement et de recherche français ou étrangers, des laboratoires publics ou privés.

1           **Importance of PCDD/F molecules' polarizability and**  
2           **steric hindrance on their adsorption onto zeolites in a**  
3           **standard EN1948-1 sampling device for incinerator**  
4                           **emission monitoring**

5   **Oliver SCHÄF<sup>1</sup>, Laurence TORTET<sup>1</sup>, Angélique SIMON-MASSERON<sup>2,3</sup>, Joël PATARIN<sup>2,3</sup>,**  
6   **Stephanie DEFOUR<sup>4</sup>, Rosine BLANC<sup>4</sup>, Christophe COSTE<sup>5</sup> and Yves ZEREGA<sup>1</sup>**

7   <sup>1</sup> Aix-Marseille Université, CNRS, MADIREL, UMR7246, Centre de Saint Jérôme, 13397 Marseille Cedex 20 (13e arrdt),  
8   France

9   <sup>2</sup> Université de Haute-Alsace, CNRS, IS2M, Axe Matériaux à Porosité Contrôlée (MPC), UMR 7361, F 68100 Mulhouse,  
10   France

11   <sup>3</sup> Université de Strasbourg, France

12   <sup>4</sup> CARSO-LSEHL, 4 Avenue Jean Moulin, 69200 Vénissieux, France

13   <sup>5</sup> Suez RV France, Tour CB21, 92040 Paris La Défense, France

14  
15   **Corresponding author:**

16   Yves ZEREGA, Aix-Marseille Université, CNRS, MADIREL, UMR7246, Centre de Saint Jérôme,  
17   13397 Marseille Cedex 20 (13e arrdt), France

18   [yves.zerega@univ-amu.fr](mailto:yves.zerega@univ-amu.fr)

19

20

21

22

## 23 **Abstract**

24 Currently, polychlorinated dibenzo-p-dioxins and polychlorinated dibenzofurans (PCDD/F)  
25 monitoring at stationary sources uses short- and long-term sampling methods compliant with EN1948  
26 standard. The XAD-2 resin is exposed to gas stream for 3-4 weeks (long term), and subsequently  
27 analysed in an accredited laboratory for 2 weeks. With the aim of developing an on-line mass  
28 spectrometer device using adsorption onto a set of different zeolites as specific adsorbents prior to  
29 mass analysis, the paper proposes to firstly test zeolites within the methods compliant with EN1948  
30 standard.

31 In addition to the non-specific external surface adsorption, zeolites possess micropores for  
32 adsorbing molecules specifically. Zeolites allowing selective adsorption of only tetra- and penta-  
33 chlorinated toxic congeners (TeCDD/F, PeCDD/F) were exposed to the gas flow of a household waste  
34 incinerator. As the extraction method of EN 1948 standard does not allow us to discern the two types  
35 of adsorption, the adsorbents have been tested at a sampling point located before the last filter. With  
36 high congener concentrations, it is expected that the dynamic adsorption properties of the zeolites can  
37 be deduced from the breakthrough of some congeners.

38 The electronic interactions between zeolite surface area and PCDD/F involve the polarizability of  
39 the molecules. Thanks to the congener breakthrough comparing two zeolite structure types, it has been  
40 deduced that toxic TeCDD/F and PeCDD/F were adsorbed in the micropores of FAU-NaX zeolite due  
41 to steric compatibility of these congeners. Moreover, the partition of congeners between the  
42 condensate and gas phase was elucidated by considering the polarizability of PCDD/F molecules.

## 43 **Keywords**

44 Zeolite; POP; PCDD/F; selective adsorbent; emission monitoring; waste incinerator

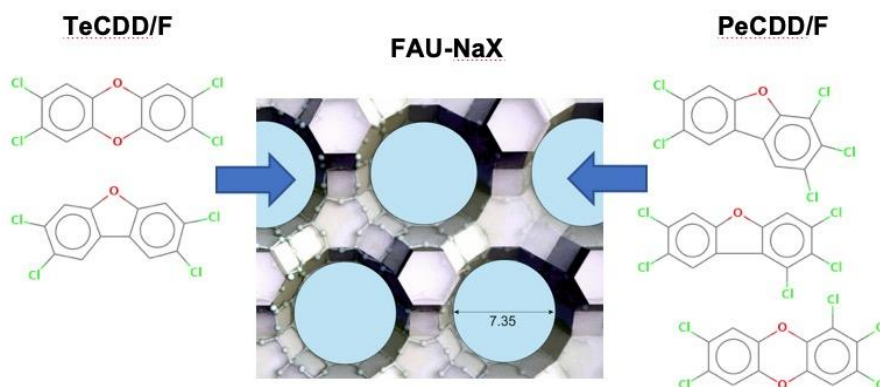
45

46

## 47 **Highlights**

- 48 • Zeolites are non-conventional adsorbent for PCDD/F adsorption
- 49 • Zeolites are exposed to incinerator gas flux
- 50 • PCDD/F polarizability governs congener partition between condensates and gas phase
- 51 • Electronic interactions between FAU-NaX and PCDD/F involve molecule polarizability
- 52 • TeCDD/F and PeCDD/F congeners are adsorbed in FAU-NaX micropores

## 53 **Graphical Abstract**



54

## 55 **1 Introduction**

56 The term “Dioxins” is often used to refer to the family of structurally and chemically related  
57 polychlorinated dibenzo-p-dioxins (PCDD) and polychlorinated dibenzo furans (PCDF). Only 17 of  
58 these (with chlorine atoms in positions 2, 3, 7 and 8) have a significant toxicity with a toxic  
59 equivalency factor (I-TEF) assigned by WHO and NATO, 2,3,7,8-TeCDD being the most toxic [1,2].

60 Waste incineration results in dioxin formation with large gas volumes released permanently.  
61 Stringent laws have been promulgated to greatly reduce dioxin emission at stationary sources because  
62 dioxins are widely distributed throughout the environment, persistent and bio-accumulated. The  
63 European Union legislation has set a limit value (ELV) of 0.1 ng/m<sup>3</sup> I-TEQ for dioxin emission from

64 waste incineration plants [3]. In Europe, monitoring of dioxin emission at stationary sources is in  
65 accordance to EN 1948 standard [4–6].

66 In 2000, Belgium was the first country worldwide which demanded the long-term sampling of  
67 dioxins in municipal waste incinerators. Then, long-term sampling has been gradually implemented.  
68 Since 2010, France has been the first country where a nation-wide legislation requires its use [7]. The  
69 gas stream is isokinetically sampled for 4-6 week period with particle- and gas-phases collected on  
70 XAD-2 resin [8–10]. This single solid support is then analysed in laboratory according to the parts 2  
71 and 3 of EN 1948 standard. The European Committee for Standardization (CEN) is currently  
72 finalising a standard for long-term sampling of PCDD/Fs and dioxin-like PCBs [11]. However, long-  
73 term sampling involves a time-integrated exposure of the adsorbent, and then off-line analysis.  
74 Consequently, short-term variation of information may be lost.

75 A continuous monitoring providing indicative dioxin levels every 8-24 hours would be relevant in  
76 term of emission transparency and incineration process control, in addition to the standard method  
77 with accurate levels of detection as reference. For instance, with the aim of designing an on-line  
78 device, the use of a set of adsorbents (such as zeolites) having different adsorption specificities  
79 according to toxicity of dioxin congeners in a sample enrichment device can increase the sensitivity  
80 level of detection of a field mass spectrometer.

81 Zeolites are adsorbents at molecular scale with large surface area and possible selective  
82 adsorption onto micropores [12–14]. Few papers relate the use of zeolite in remediation of dioxins  
83 from incineration gases [15–18]. Jäger *et al.* demonstrated a selective adsorption of dioxins onto  
84 zeolites, with dioxins thermally desorbed from incineration ashes [19]. Adsorption properties of  
85 dioxins onto zeolites and energy of desorption were determined by temperature programmed  
86 desorption (TPD) due to dioxin low volatility [20–24].

87 Authors of this study have proposed to determine the adsorption properties of zeolites with  
88 solutions of dioxins in isoctane. Adsorption isotherms showed that 2,3-DCDD has been adsorbed in  
89 the micropores of FAU-NaX zeolite with very high affinity, regarding the adsorbent micropore size  
90 and dynamic molecule size, while the adsorption of 1,2,3,4-TeCDD has been limited to the external

91 surface [25]. Furthermore, the authors explained that the nature of the charge compensating cations  
92 could have an influence on the congener adsorption in the micropores [26]. The exchange of  $\text{Na}^+$   
93 cation by trivalent cation  $\text{La}^{3+}$  in FAU-type X-zeolites has led to the adsorption of 1,2,3,4 TeCDD  
94 [27,28].

95 Besides the size compatibility, the electronic interactions play a key role in adsorption. The toxic  
96 PCDD/F congeners possess quadrupolar moments and large polarisabilities inducing electrostatic and  
97 dispersion interactions responsible of the interactions with the aryl hydrocarbon receptor (AhR) with  
98 regards to their specificity of interaction and toxicity [29–34]. Same electronic interactions should be  
99 involved for toxic PCDD/F congeners adsorption onto zeolites. Dispersion interactions also occur for  
100 the adsorption of polarisable solvents [35]. Isooctane adsorption onto FAU-NaX zeolite has been  
101 demonstrated by authors of this study using Thermal Gravimetric Analysis and DNP RMN  
102 Spectroscopy with the addition of a polarization-transfer agent [28]. Hence the micropore accessibility  
103 can be greatly enhanced using PCDD/F in the presence of isooctane.

104 Thermal-desorption is a relative simple method to recover compounds from adsorbents of a  
105 sample enrichment device, for instance. Zeolites have good mechanical and thermal stabilities, so that  
106 they can be heated at high temperatures to ensure that the adsorbent is free of contamination prior to  
107 sampling and to recover the greater number of adsorbed molecules for subsequent identification and  
108 quantification. However, in the case of sampling at incineration process, a degradation mainly by  
109 dechlorination and dioxin formation could occur at temperatures higher than 300 °C due to the  
110 presence of ashes and other compounds in the adsorbents [36]. As a consequence, false levels of  
111 dioxin could be detected.

112 Recently, in a laboratory-scale experiment, authors of this study have shown a low effectiveness  
113 of the gas-phase dioxin adsorption onto faujasite beads at room temperature. It was mainly due to the  
114 large bead diameter reducing micropore accessibility. A new recipe to synthesise beads with smaller  
115 diameters has been then proposed by authors of this study. These beads have mechanical performances  
116 high enough for implementation in an on-line adsorption process [37]. The beads should be able to  
117 sustain the load they will be subjected to gas sampling at full-scale in an incineration process.

118 In this paper, two structure types of zeolite with two bead diameters have been exposed to gas  
119 fluxes of a waste-to-energy plant in a sampling device compliant with EN 1948-1 standard. The  
120 sampling device has been modified so that two different adsorbents can be tested in parallel with the  
121 same gas fluxes and a breakthrough be measured. The toxic congener concentrations adsorbed by the  
122 adsorbents have then been measured by a certified laboratory using the methods of EN 1948 standard.  
123 The adsorption properties of the zeolites have been then determined taking into account the electronic  
124 interactions between the materials and toxic PCDD/F congeners.

## 125 **2 Materials and Methods**

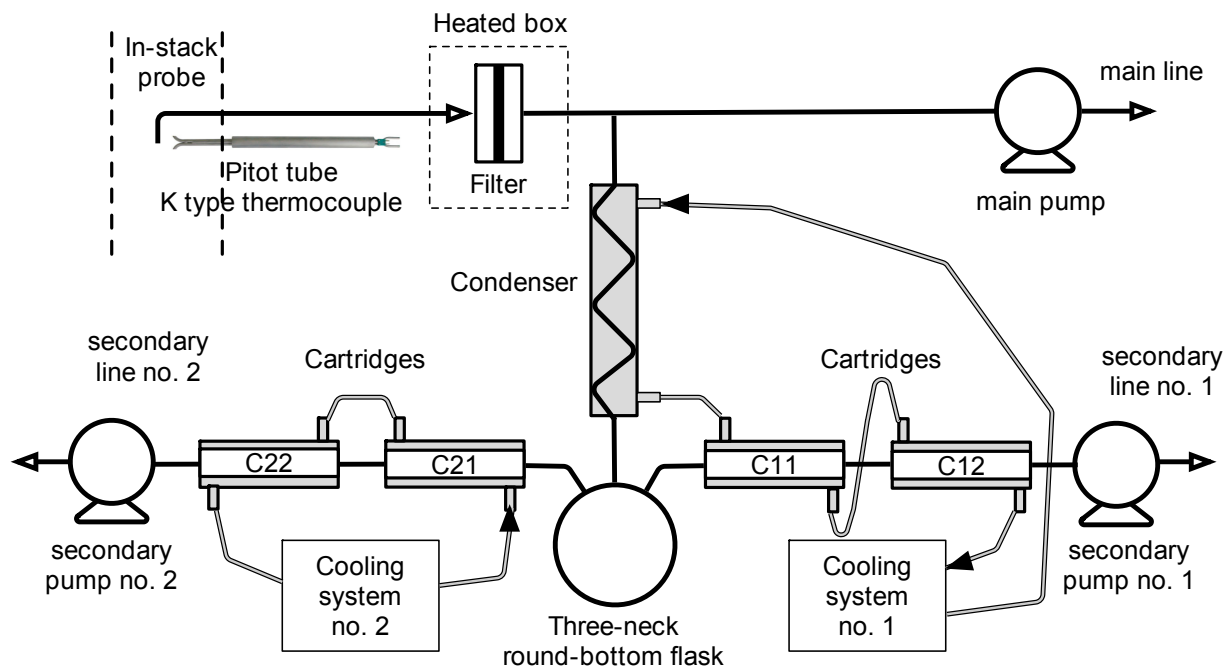
### 126 **2.1 Preparation of zeolite beads**

127 Powder of FAU-NaX (octahedron micro-crystal of 2-3  $\mu\text{m}$ ) and of \*BEA-H (nano-crystal agglomerate  
128 of 2  $\mu\text{m}$ ) have been purchased from Sigma-Aldrich® and Clariant®, respectively. \*BEA-H zeolite has  
129 been partly ion-exchanged with Na cations leading to \*BEA-Na.

130 The beads have been obtained by shearing the zeolite powder in the presence of water and sodium  
131 metasilicate as inorganic binder (5 wt %). The two zeolite structures have been used for gas sampling  
132 in various bead sizes: FAU-NaX beads of 0.5-0.8 mm in diameters, FAU-NaX beads of 0.25-0.4 mm  
133 in diameters and \*BEA-Na beads of 0.25-0.4 mm in diameters.

### 134 **2.2 Sampling device**

135 The sampling device refers to EN 1948-1 standard [4] using the filter/condenser method, with flow  
136 division and solid adsorbent downstream of the condenser. This sampling method ensures a constant  
137 flow in adsorbent even if the flow of the main line varies. The base of the device is a continuously dust  
138 sampling train from a gas duct under isokinetic conditions (from Cleanair Europe, La Penne-sur-  
139 Huveaune, France). A special glassware set (from La Verrerie Villeurbannaise, Villeurbanne, France)  
140 completes the dust sampling train, comprising XAD-2 resin cartridge, condenser, condensate container  
141 and different connectors and lines.



142

143 Fig. 1: Sampling train and adaptation of the glassware set for testing adsorption with selective  
 144 materials according to EN 1948-1 standard. The cartridges C11 and C21 are filled with the testing  
 145 adsorbents; the cartridges C12 and C22, or backup cartridges, are filled with XAD-2 resin.

146 The sampling probe is heated and equipped with a Pitot tube and K type thermocouples (Fig. 1).  
 147 Particles are collected on a filtration media placed in a heated box. The sample flow rate is adjusted by  
 148 means of the pumps in the main and secondary lines. The glassware set is modified for testing of  
 149 zeolite adsorption properties. A second gas-sampling line with adsorbent cartridge is added in parallel  
 150 with the first one, requiring a three-neck balloon for recovering condensate. It is then possible to  
 151 compare adsorption properties of two different materials with the same incineration gas flux.  
 152 Furthermore, each line has two adsorbent cartridges in series: the first cartridge is filled with the  
 153 testing adsorbent, while the second, filled with XAD-2 resin, is the backup cartridge for PCDD/F  
 154 breakthrough determination. In each line after the cartridges, a secondary pump (denoted as secondary  
 155 pumps no. 1 and 2) aspirates the gas through a drying line filled with silica gel and a counter measures  
 156 the volumetric flow rate of dry gas. The first cooling system supplies the condenser and the jackets of  
 157 the both cartridges of the secondary line no. 1. An additional cooling system supplies the both  
 158 cartridges of the secondary line no. 2. The temperatures of the cooling devices have been adjusted so  
 159 that the temperatures of the first cartridges of lines no. 1 and 2 are identical. However, a discrepancy  
 160 has been observed: higher temperature has been measured in cartridge C11 than in cartridge C21.



### 161 2.3 Sampling campaign

162 Sampling campaign has been performed in the same waste-to-energy plant for 3 days. Therefore, the  
163 samplings are denoted as: D1, D2 and D3. SUEZ Environnement (France), as delegated owner of the  
164 waste-to-energy plant, has coordinated the campaigns. The waste-to-energy plant is equipped with one  
165 line including: electrostatic precipitator (ESP), fabric filter (FF) and DeNOx catalyst (for instance, see  
166 ref. [38]). Typically, the incinerator gas fluxes are sampled in a long straight vertical section of tubing  
167 (in the stack). In this study, the sampling point has been chosen between the ESP and FF in order to  
168 reach high concentrations of congeners. This is an unusual place with a turbulent stream flow. As a  
169 consequence, measurement is not representative of the particle phase and of dioxin concentrations  
170 emitted by incinerator, even with isokinetic sampling [39]. However, with high concentrations of  
171 PCDD/F congeners, the breakthrough of certain congeners must occur with the adsorbents.

172 The glass cartridges C11 and C21 have been filled with 30 g of beads of zeolites as follow: for  
173 D1 sampling, with XAD2 and with FAU-NaX beads of 0.5-0.8 mm diameters; for D2 sampling, with  
174 FAU-NaX beads of 0.25-0.4 mm diameters and with FAU-NaX beads of 0.5-0.8 mm diameters; and  
175 for D3 sampling, with FAU-NaX beads of 0.25-0.4 mm diameters and with \*BEA-Na beads of 0.25-  
176 0.4 mm, respectively. After packing, the zeolites have been conditioned: they have been heated to 300  
177 °C under a nitrogen stream and kept at these conditions for about 24 h. The backup cartridges C12 and  
178 C22 have been filled with 30 g of XAD-2 resin. XAD-2 has a particle size of 20-60 mesh (*i.e.* 0.25-  
179 0.84 mm) with an apparent porosity between the grains (90 Å mean pore size). Then, the adsorbents  
180 have been spiked with PCDD/F standards (a mixture of <sup>13</sup>C-labelled toxic PCDD/F in toluene) before  
181 exposition to the incineration gas flux.

182 All of the samples have been collected for 6 hours. The volumetric flow rates have been  
183 maintained constant during sampling and compliant with the isokinetic conditions required by EN  
184 1948 standard. The sampled volumes have been measured 3-3.1 m<sup>3</sup> in the main line and 2-2.7 m<sup>3</sup> in  
185 the two secondary lines with 13-15 % moisture, depending on the sampling day. The inlet temperature  
186 of the bulk gases at the probe has be measured at almost 198 °C, while in the filter box the temperature  
187 at 110 °C. The ice water has circulated at 2-5 °C in the jackets of the condenser and cartridges.

188 **2.4 Concentration measurement**

189 The glassware set, condensates and adsorbent supports have been then analysed in CARSO laboratory  
190 according to parts 2 and 3 of EN 1948 standard. A solution of <sup>13</sup>C-labelled PCDD/F has been injected  
191 on adsorbents before extraction. The toxic PCDD/F have been Soxhlet extracted with toluene from  
192 adsorbents. The extract has been purified on silica/modified silica and alumina columns. Quantitative  
193 analysis has been performed by isotopic dilution on high-resolution gas chromatograph/mass  
194 spectrometer Autospec ULTIMA from Waters [40].

195 The PCDD/F concentration (ng/Nm<sup>3</sup>) has been calculated from the PCDD/F quantity (ng)  
196 measured in the filter, condenser and cartridge divided by the sampled volume of gas. However, we  
197 are not allowed to disclose the true values of concentrations. It is for that reason that they are expressed  
198 in  $\alpha$  ng/m<sup>3</sup>, keeping the same value for  $\alpha$  to be able to make comparisons between absolute quantities  
199 adsorbed onto zeolites.  $C_C(c)$  and  $C_P(c)$  are the concentrations of congener  $c$  measured in the  
200 condensate and in the particulate phase, respectively. The concentration denoted as  $C_G(c)$  is the  
201 concentration of congener  $c$  in the gas phase and corresponds to the sum of the concentrations  
202 measured in the four adsorbent cartridges. The total concentration of congener  $c$  is calculated from:  
203  $C_T(c) = C_P(c) + C_C(c) + C_G(c)$ .

204 **3 Results and Discussion**

205 **3.1 Testing the analytical method**

206 The limit of detection (LOD) and limit of quantification (LOQ) have been determined as described in  
207 EN 1948-2 §3.8 and 3.9 by using the mean analytical blank plus  $x$  times the standard deviation of the  
208 analytical blank (Tab. 1). A concentration value that falls between the LOD and LOQ is assigned the  
209 value of the LOQ. A concentration value that falls below the LOD is assigned a value of zero.

210 The percent uncertainty of measured quantity for each toxic congener has been calculated  
211 using NF ISO 11352 standard [6].

212 The recovery rates of <sup>13</sup>C-labelled PCDD/F standards from XAD-2 resin and three different  
 213 used zeolites have been compared (Tab. 1). The recovery rates have been almost identical and  
 214 sufficiently high to be accepted. This result proves Soxhlet extraction method using toluene as the  
 215 extraction solvent can be applied to zeolites.

216 Tab. 1: Limit of detection (LOD), limit of quantification (LOQ), blank, uncertainty and examples of  
 217 recovery rates of PCDD/F toxic congeners from XAD-2 and zeolites. The sampling volumes can be  
 218 different, however the values of LOD and LOQ are independent of the sample volume according to  
 219 calculation.

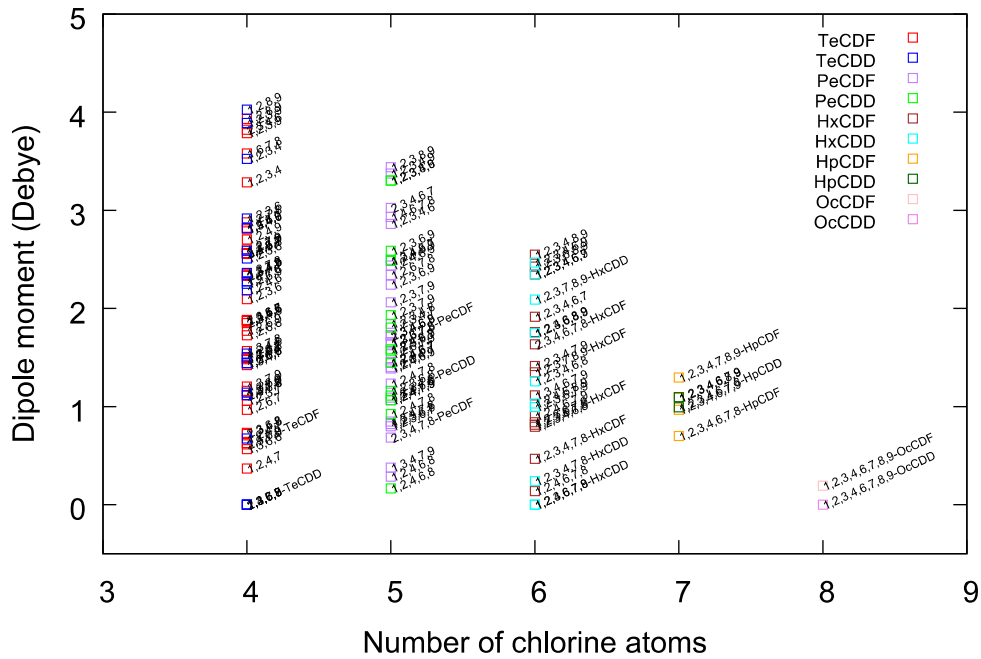
220 (\*) A concentration value that falls between the LOD and LOQ is assigned the value of the LOQ. (\*\*)  
 221 A concentration value that falls below the LOD is assigned a value of zero. (\*\*\*) For instance, D3-  
 222 C11 stands for sampling D3 and cartridge C11 according to Fig. 1.

PCDD/F	LOD (pg per sample)	LOQ (pg per sample)	Blank (ng per sample)	Uncertainty (%)	Recovery rate D1-C21 (***) XAD-2 (%)	Recovery rate D3-C11 (***) FAU-NaX beads of 0.25-0.4 mm diameters (%)	Recovery rate D2-C21 (***) FAU-NaX beads of 0.5-0.8 mm diameters (%)	Recovery rate D3-C21 (***) *BEA-Na beads of 0.25-0.4 mm diameters (%)
2,3,7,8-TeCDD	0.83	1.2	<0,00120 (**)	30	95	98	94	92
1,2,3,7,8-PeCDD	0.81	1.2	<0,00120 (**)	30	81	78	81	95
1,2,3,4,7,8-HxCDD	1.1	1.5	<0,00150 (**)	30	89	79	84	79
1,2,3,6,7,8-HxCDD	1.1	1.5	<0,00150 (**)	40	80	74	78	75
1,2,3,7,8,9-HxCDD	1.1	1.5	<0,00150 (**)	60	-	-	-	-
1,2,3,4,6,7,8-HpCDD	3.9	10	<0,01000 (*)	30	89	80	83	87
OcCDD	13	25	<0,02500 (*)	60	64	61	64	75
2,3,7,8-TeCDF	1.0	1.5	<0,00150 (**)	40	84	82	82	80
1,2,3,7,8-PeCDF	0.68	1.2	<0,00120 (**)	30	86	76	56	71
2,3,4,7,8-PeCDF	0.70	1.2	<0,00120 (**)	30	75	71	73	85
1,2,3,4,7,8-HxCDF	0.71	1.2	<0,00120 (**)	30	84	78	80	73
1,2,3,6,7,8-HxCDF	0.73	1.2	<0,00120 (**)	30	88	81	82	78
2,3,4,6,7,8-HxCDF	0.72	1.2	<0,00120 (**)	30	93	84	88	83
1,2,3,7,8,9-HxCDF	0.81	1.5	<0,00150 (**)	30	81	70	50	68
1,2,3,4,6,7,8-HpCDF	2.2	5.0	<0,00500 (**)	30	69	73	72	81
1,2,3,4,7,8,9-HpCDF	0.84	1.5	<0,00150 (**)	30	88	74	60	50
OcCDF	3.9	10	<0,01000 (**)	30	65	57	61	63

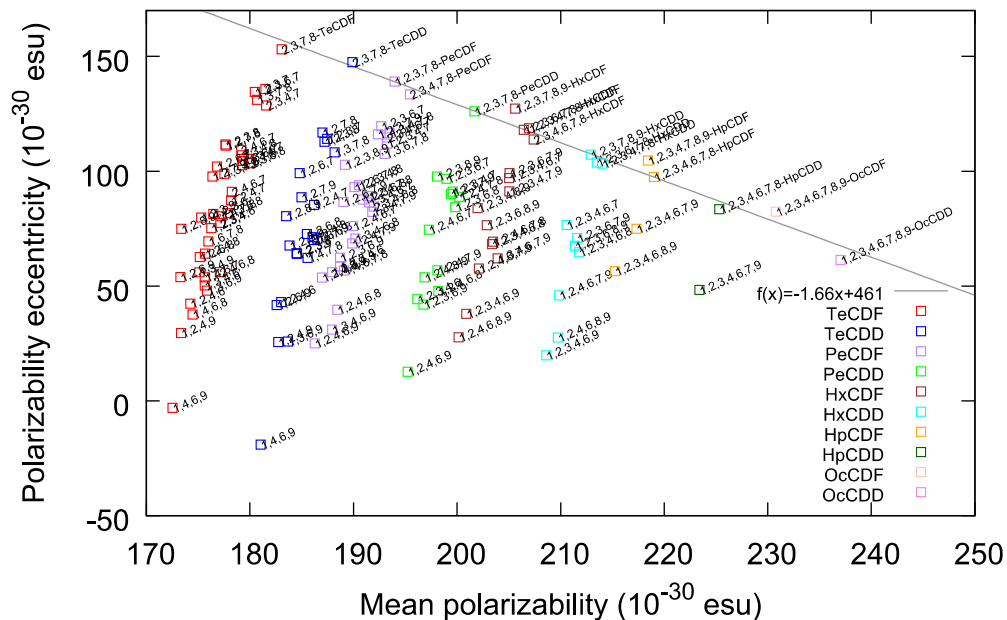
223

### 224 3.2 Spatial structure and electrical properties of PCDD/F

225 Prior to sampling result interpretation, the spatial structure and electrical properties of PCDD/F must  
 226 be developed. PCDD/F are quasi-planar molecules in the x0y plane, with the long axis aligned along  
 227 the x-direction. The molecule size in the y-direction defines the steric compatibility with the zeolite  
 228 micropore diameter sizes for specific adsorption. For instance, the molecule sizes in the y-direction  
 229 are: 7.4 Å for DD, DF, 2,3,7,8-TeCDF and 2,3,7,8-TeCDD; 8.6 Å for 1,2,3,7,8-PeCDD, 1,2,3,7,8-  
 230 PeCDF and 2,3,4,7,8-PeCDF; and 9.9 Å for OcCDD and OcCDF [19,41].



231



232

233 Fig. 2: (top graph) Dipole moment as a function of the number of chlorine atoms and (bottom graph)  
 234 mean polarizability as a function of polarizability eccentricity of tetra- to octa-chlorinated PCDD/F  
 235 congeners. The plotted values are simulated values obtained with same simulation tools and collected  
 236 from data tables of ref. [32,42,43]. The values of the toxic congeners have been linearly interpolated  
 237 by the straight line of equation:  $y = -1.66x + 461$ . In both graphs, the toxic congeners are  
 238 referenced by their full name, e.g. 2,3,7,8-TeCDD, while the non-toxic by the position of the chlorine  
 239 atoms merely, e.g. 1,2,3,4.

240 Gu *et al.* have examined the electronic interactions between PCDD/F and AhR to establish the  
 241 main factor in predicting the PCDD/F toxicology [32,43]. They have determined the electronic  
 242 structures of all the PCDD/F using ab initio quantum chemical calculations. Then the polarizability

243 values have been calculated using the Density Functional Theory (DTF) and optimized globally  
244 without any *a priori* symmetry. Concomitantly, the values of the dipole moment have been calculated  
245 by Yang *et al.* using the same methods and tools [42]. From these simulation results, it is then possible  
246 to have a set of comparable values of the dipole moment and polarizabilities for all toxic and non-toxic  
247 PCDD/F congeners (Fig. 2). The electric polarizability tensor of toxic PCDD/F is quasi-diagonal with  
248 diagonal terms denoted as:  $\alpha_{xx}$ ,  $\alpha_{yy}$  and  $\alpha_{zz}$  in the x-, y- and z-directions, respectively. The mean  
249 polarizability is expressed as:  $\bar{\alpha} = \frac{1}{3}(\alpha_{xx} + \alpha_{yy} + \alpha_{zz})$  and polarizability eccentricity in the plane  
250 x0y as:  $\epsilon = \alpha_{xx} - \alpha_{yy}$ . For the toxic PCDD/F the diagonal term  $\alpha_{zz}$  ranges over low values (from 63  
251 to 79 x10<sup>-30</sup> esu), as the molecules are quasi-planar.

252 In Fig. 2, the toxic congeners are referenced by their full name, *e.g.* 2,3,7,8-TeCDD, while the  
253 non-toxic ones by the position of the chlorine atoms merely, *e.g.* 1,2,3,4. The dipole moment and  
254 polarizability units are expressed in Debye and electrostatic unit (esu), respectively, where esu is  
255 expressed as 1.112 x 10<sup>-16</sup> C<sup>2</sup> x m<sup>2</sup> x J<sup>-1</sup> in terms of CGS units.

256 Only the polarizability could separate toxics from non-toxics of each family, as the toxic isomers  
257 have higher polarizabilities than the non-toxic ones. The differences of polarizability eccentricity  
258 between toxics and non-toxics are higher than those of mean polarizability. The polarizability values  
259 of the toxic congeners can be interpolated in the system of coordinates "mean polarizability" and  
260 "polarizability eccentricity" by the straight line of equation:  $y = -1.66x + 461$  (Fig. 2). As a  
261 consequence, the polarizability of the toxic congeners increases quasi-linearly when the volume  
262 occupied by electrons increases, while the polarizability eccentricity decreases (from TeCDD/F to  
263 OcCDD/F congeners).

264

265

266

267

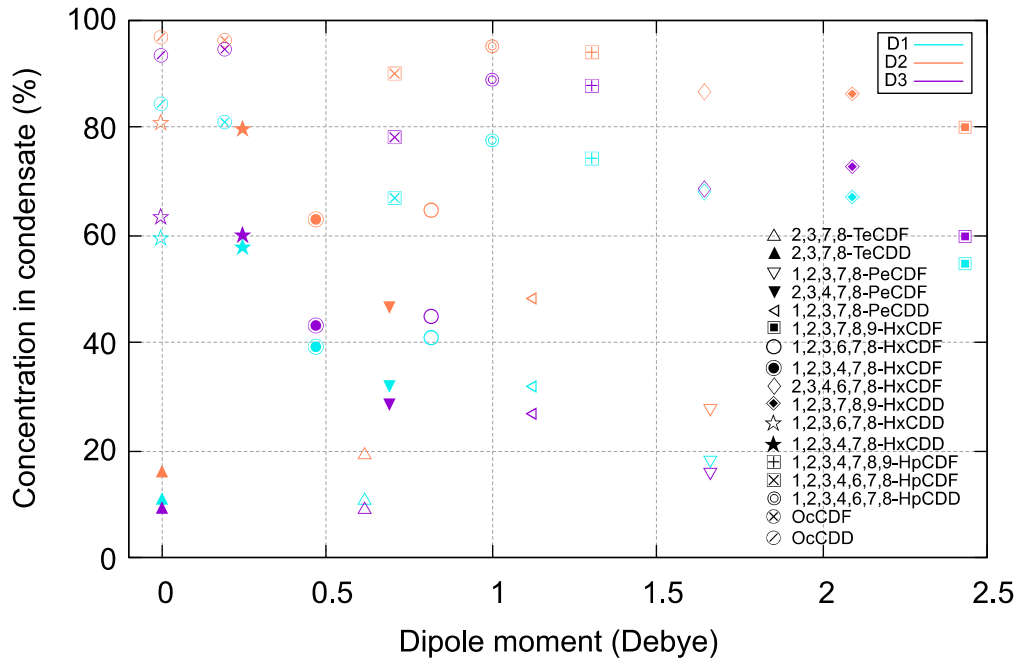
### 268 3.3 PCDD/F concentration in the condensates

269 Similar concentrations of the toxic congeners have been measured in the particulate phase,  
270 condensates and gas phase for the samplings D1 and D2, while for the sampling D3 the concentrations  
271 have been twice higher for more than half of the congeners. The toxic congeners have been measured  
272 in negligible quantities in the particulate phase.

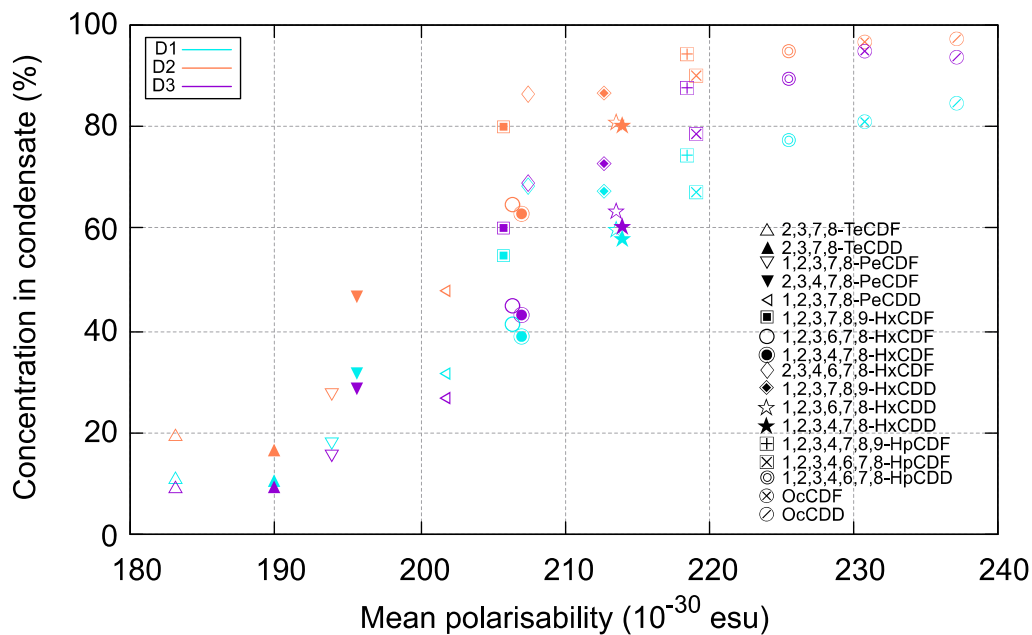
273 The relative concentrations of toxic PCDD/F measured in the condensates,  $C_C(c)(\%) = 100 \times$   
274  $\frac{C_C(c)}{C_T(c)}$ , are plotted as a function of the dipole moment and mean polarizability of the congeners (Fig. 3).  
275 The relative quantities trapped in the condensates increase with the number of chlorine atoms of the  
276 congeners, from 10-20 % for TeCDD/F to 85-95 % for OcCDD/F. Quasi-similar relative  
277 concentrations have been measured for the samplings D1 and D3 while for the sampling D2, the  
278 relative concentrations are slightly higher for all the congeners. This is due to different temperatures of  
279 the ice water supplied by the cooling system no. 1 measured at 5 °C for the samplings D1 and D3 and  
280 at 3 °C for the sampling D2.

281 Consequently, the relative concentrations in the condensates and gas phase depend on the  
282 temperature in the condenser. The heat transfers between the ice water and molecules in the gas flow  
283 depend on the volumetric flow rate of the gas. To a lesser extent, the volumetric flow rate could  
284 influence the measured quantities. Reproducible relative concentrations in both the condensates and  
285 flow passing through the adsorbents can be achieved by maintaining constant the values of the  
286 operating parameters. The ratio of PCDD/F concentrations measured in the condensates and gas phase  
287  $p(c) = \frac{C_C(c)}{C_G(c)}$  is sampling device dependant and can be estimated from some samplings. Insuring same  
288 operating conditions, the emitted total concentration can be then calculated from the concentration  
289 measured only in the adsorbent by:  $C_T(c) = C_G(c) + C_C(c) = C_G(c)(1 + p(c))$ .

290



291



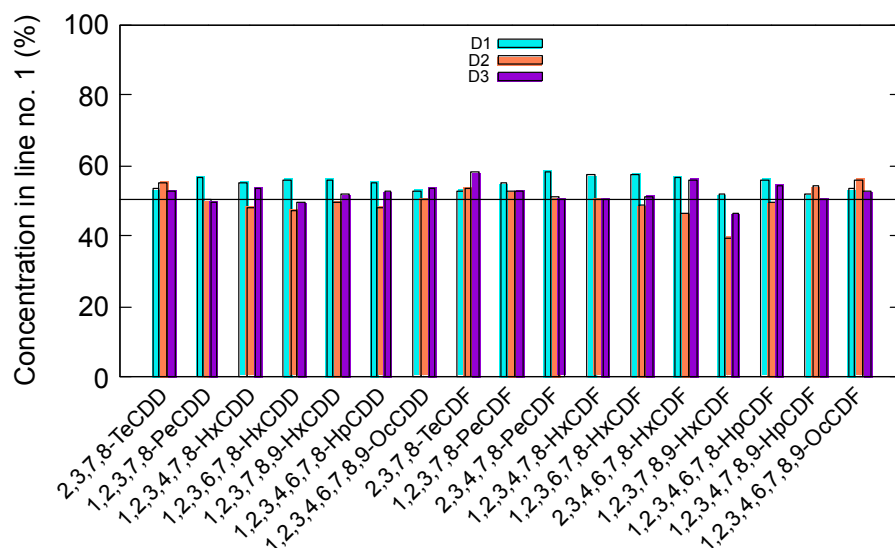
292

293 Fig. 3: Relative concentrations of toxic PCDD/F measured in the condensate for the samplings D1, D2  
 294 and D3 as a function of (top graph) dipole moment and (bottom graph) mean polarizability.

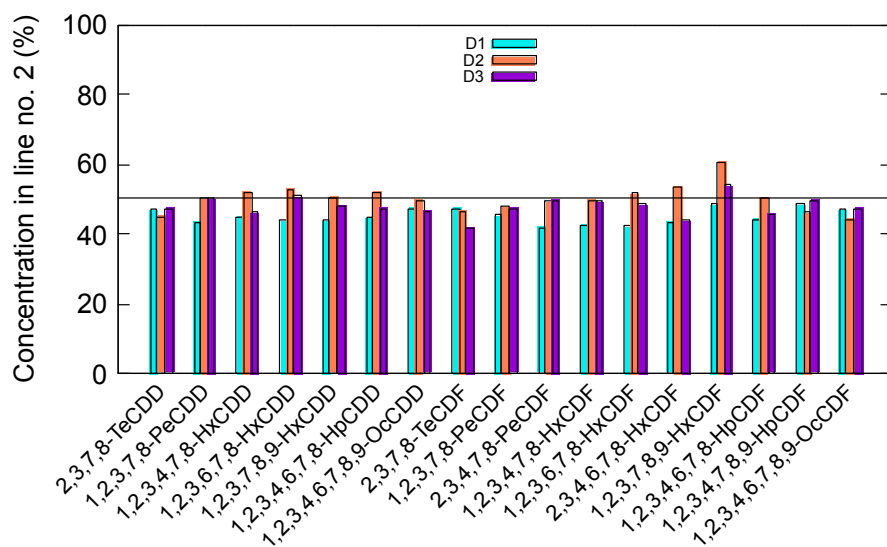
295 Furthermore, on the one hand, no relations can be deduced between the relative concentrations of  
 296 toxic PCDD/F measured in the condensate and the values of the dipole moment (top graph of Fig. 3).  
 297 On the other hand, the interaction between the PCDD/F and water in the condenser mainly depends on  
 298 the PCDD/F polarizability (bottom graph of Fig. 3). The more the congener polarisable, the more the

299 congener adsorbed by physisorption by water droplets falling then by gravity into the condensate  
 300 flask. Induced dipole-permanent dipole interaction exists between PCDD/F congeners and water.

301 **3.4 PCDD/F concentration in the two gas lines**



302



303

304 Fig. 4: Relative concentrations of toxic PCDD/F measured in secondary lines no. 1 (top graph) and 2  
 305 (bottom graph) for the samplings D1, D2 and D3.

306 The relative concentrations in the gas lines no. 1 and 2 have been calculated from the relations:

307  $C_{L1}(c)(\%) = 100 * \frac{C_{G11}(c)+C_{G12}(c)}{C_G(c)}$  and  $C_{L2}(c)(\%) = 100 * \frac{C_{G21}(c)+C_{G22}(c)}{C_G(c)}$ , respectively, with for



308 instance,  $C_{G21}(c)$  the concentration of congener  $c$  measured in the adsorbent packed in the first  
309 cartridge of the secondary line no. 2. The comparison of the values measured between the two  
310 secondary gas lines shows an acceptable measurement reproducibility (Fig. 4). The slight discrepancy  
311 between the two lines is due to a temperature difference between the two line inlets. The higher the  
312 temperature, the higher the concentration in the line.

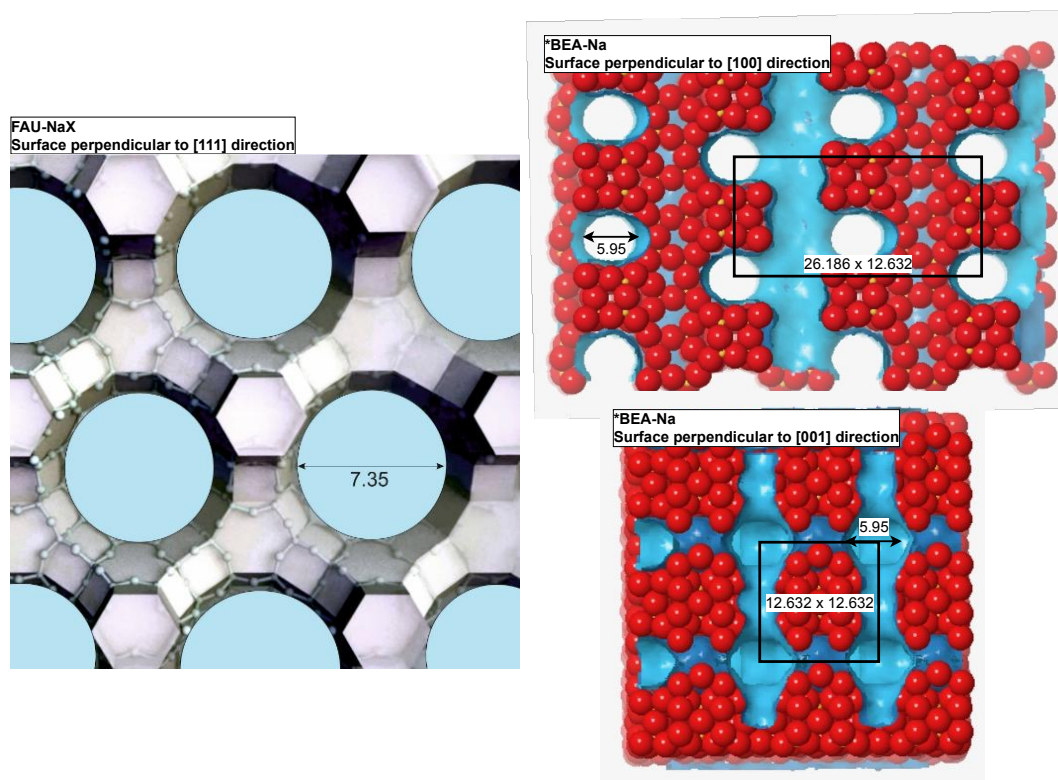
### 313 **3.5 Zeolite structure types**

314 Prior to adsorption result interpretation onto zeolites, their structure types and adsorption properties  
315 must be discussed. Zeolites are microporous crystalline aluminosilicate solids. Their inorganic  
316 framework (Si-O-Al) can be described as an assembly of  $TO_4$  tetrahedra for which T stands for silicon  
317 or aluminium atoms and each oxygen atoms, located at the vertices, is shared by two tetrahedra. These  
318 assemblies design channels and/or cavities of molecular dimensions with precisely defined sizes [14].  
319 These arrangements define structure types. Two zeolite structure types have been submitted to gas  
320 flux: FAU-NaX and \*BEA-Na. FAU-NaX has supercages of tetrahedral symmetry of 11.24 Å in  
321 diameter with interconnectivities (micropores) of 7.35 Å in diameter. The size of micropore apertures  
322 of \*BEA-Na is 6.68 Å in diameter and micropore cavity 5.95 Å.

323 FAU-NaX and \*BEA-Na crystallize in cubic and tetragonal unit cells, respectively. Confirmed by  
324 TEM imaging [44,45], the outer surface area of micro crystals (giving the external surface area and  
325 external porosity) of FAU-NaX and \*BEA-Na can be represented for the three directions of the  
326 coordinate system by: for FAU the surface perpendicular to [111] direction, and for \*BEA surfaces  
327 perpendicular to [100], [010] and [001] directions, respectively. As for a tetragonal crystal system,  
328 zeolite \*BEA surfaces perpendicular to [100] and [010] directions are identical.

329 The external surface roughness and porosity of a FAU-NaX crystal perpendicular to [111]  
330 direction (from Clarian® youtube video) and those of \*BEA-Na crystal perpendicular to [100] and  
331 [001] directions (from the web tool provided by the database of the International Zeolite Association  
332 [46]) are shown in Fig. 5. For \*BEA-Na, the red balls represent the oxygen atoms of the framework

333 Si-O-Al on the external surface, and the internal surface areas of the micropores are represented in  
334 blue.



335  
336 Fig. 5: External surface roughness and porosity of a FAU-NaX crystal perpendicular to [111] direction  
337 (left) and \*BEA-Na crystals perpendicular to [100] or [010] (right top) and [001] directions (right  
338 bottom). The pictures are extracted from Clarian® youtube video for FAU and web tool of ref. [46]  
339 for BEA. Note that for the FAU (111) surface the 1 x 1 surface repeat unit is 17.13 x 17.13 Å [47] in  
340 contrast to the cubic 24.35 Å unit cell dimensions.

341 According to [47] the outer surface of FAU-NaX octahedral crystals comprise partially the walls  
342 of the super cages but also sodalite cages and 6 membered rings which contribute to the surface  
343 roughness. Probably those of \*BEA nano crystals do show walls of the micropore channels that are  
344 parallel to the outer surface. The external surface of both zeolites is an oxygen-terminated,  
345 hydroxylated and partially water saturated polar surface (see scheme 1 showing interaction between  
346 adsorbed DD dioxin and zeolite in ref. [24]). So, it can be assumed that the outer surfaces of both  
347 crystals have quasi-identical physical-chemical properties.

348

349

### 350 **3.6 Adsorption of PCDD/F onto zeolite beads**

351 The adsorption of PCDD/F onto zeolites can be summarized by: (1) non-selective adsorption of the  
352 whole of the congeners onto the external surface and (2) specific adsorption into the micropores of the  
353 zeolites, when the steric hindrance is limited so only certain congeners can enter the micropores.

354 Not any of the PCDD/F congeners can enter the micropores of the \*BEA-Na. The micropore size  
355 of FAU-NaX allows only the admission of 2,3,7,8-TeCDD and 2,3,7,8-TeCDF congeners among the  
356 toxic congeners. The toxic PeCDD/F isomers can be only adsorbed at the micropore entrances of  
357 FAU-NaX, thus blocking the access to the remainder of the micropore volume of the crystal.

358 When the beads are packed in a cartridge, it exists a macroporosity between the beads, in addition  
359 to the one between the crystals and binder in each bead, where the gas can pass through. However, it  
360 can be assumed that the main interactions between the gas and zeolites occurs on the external surface  
361 area of the beads, as gas velocity is higher inside the macroporosity of the bead due to higher flow  
362 hindrances. In consequence, the same adsorption properties are expected for the external surface area  
363 of \*BEA-Na and FAU-NaX beads of identical diameter.

364 With the best arrangement of spherical beads packed in a given volume of the cartridge, when the  
365 bead diameter is doubled, the surface area of all the beads is divided by 2 and the weight of the beads  
366 does not change. As a consequence, the micropore accessibility is divided by two, if it is assumed that  
367 the interactions between the gas flow and zeolite occur mainly on the external surface area of the  
368 beads.

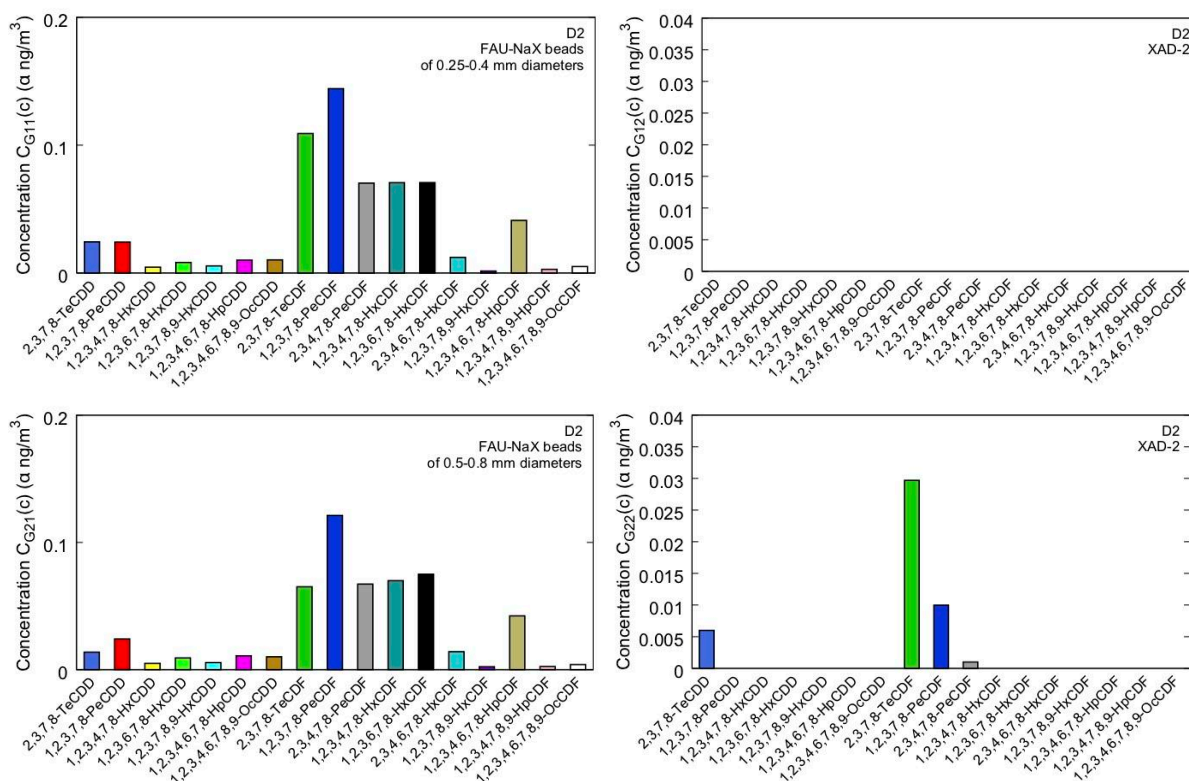
369 Authors of this study have characterised the synthesized zeolite beads used in the sampling  
370 device. Nitrogen adsorption-desorption isotherms have been performed at 77 K with Micromeritics  
371 ASAP 2420 MP Instruments. Before each measurement, the samples have been outgassed to a residual  
372 pressure of less than 0.8 Pa at 150 °C for 15 h for the beads. Specific surface area, denoted as  $S_{\text{BET}}$ , has  
373 been calculated according to the BET method ( $10^{-6} < p/p^0 < 0.05$ ) and compared to external surface,  
374 denoted as  $S_{\text{ext}}$ , associated to intra- and inter-particle mesoporosities [48]:  $S_{\text{BET}}$  is equal to 700 and  
375 410 m<sup>2</sup>/g, and  $S_{\text{ext}}$  to 5 and 100 m<sup>2</sup>/g for FAU-NaX (beads of 0.25-0.4 mm in diameters) and \*BEA-Na  
376 (beads of 0.25-0.4 mm in diameters), respectively. The external surface of \*BEA-Na beads is 20 times

377 larger than those of FAU-NaX beads, as the external surface of \*BEA-Na beads is composed of the  
 378 surface of the nano-crystals, mesoporosity between the nano-crystals of agglomerates and  
 379 macroporosity between the agglomerates, while the external surface of FAU-NaX beads is limited to  
 380 the surface of the micro-crystals and macroporosity between the micro-crystals

### 381 3.7 PCDD/F concentration adsorbed onto zeolites

382 The concentrations of toxic congeners adsorbed onto FAU-NaX beads of 0.25-0.4 mm and 0.5-0.8  
 383 mm diameters for the sampling D2 are given in Fig. 6. The breakthrough of 2,3,7,8-TeCDD/F,  
 384 1,2,3,7,8-PeCDF and 2,3,4,7,8-PeCDF has occurred with the beads of 0.5-0.8 mm diameters. The  
 385 same congener quantities have been measured in the two gas lines, when the concentrations of the first  
 386 and second cartridges are added.

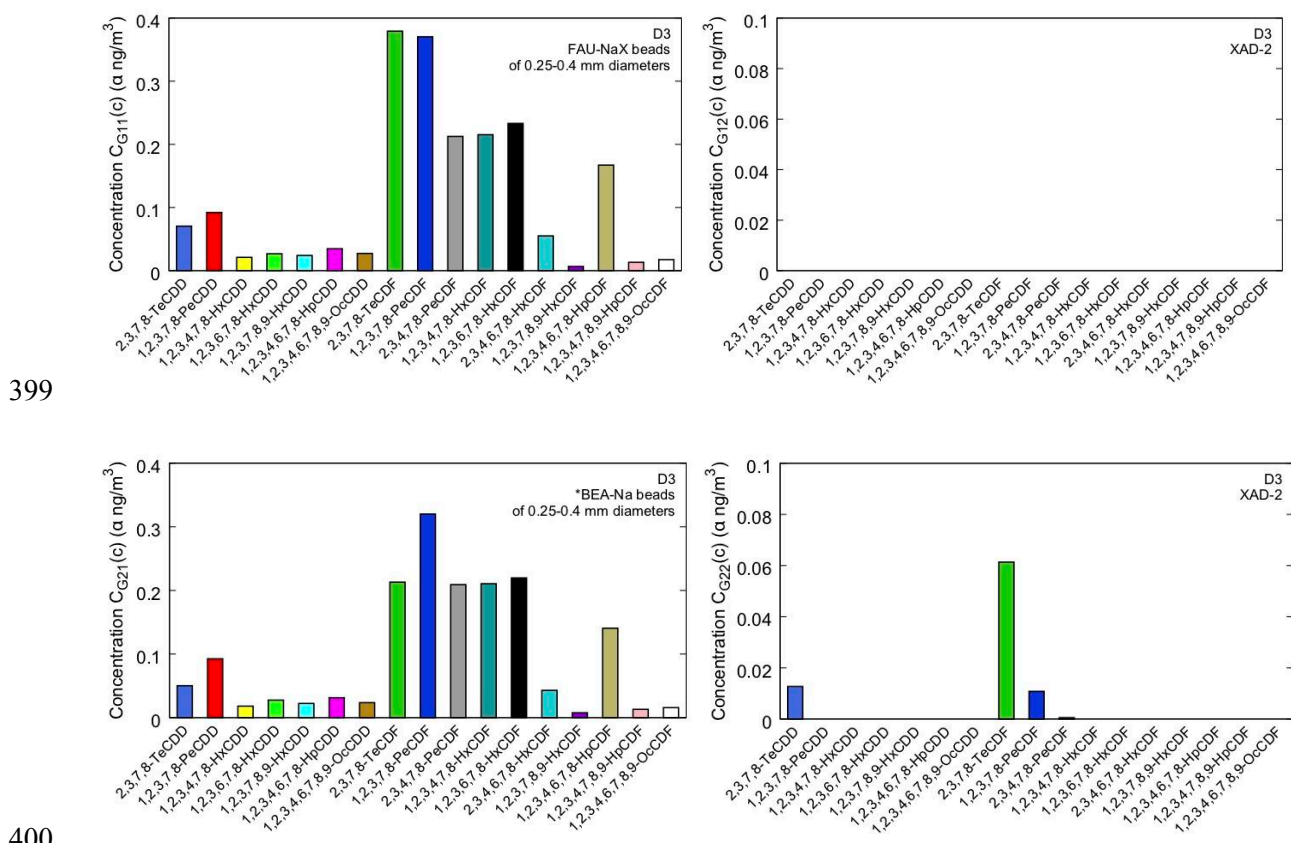
387



388

389 Fig. 6: Concentrations of toxic PCDD/F adsorbed the sampling day D2 in cartridges packed with  
 390 FAU-NaX beads of 0.25-0.4 mm diameters and XAD-2, respectively (top figures, line no. 1) and in  
 391 cartridges packed with FAU-NaX beads of 0.5-0.8 mm diameters and XAD-2, respectively (bottom  
 392 figures, line no. 2).

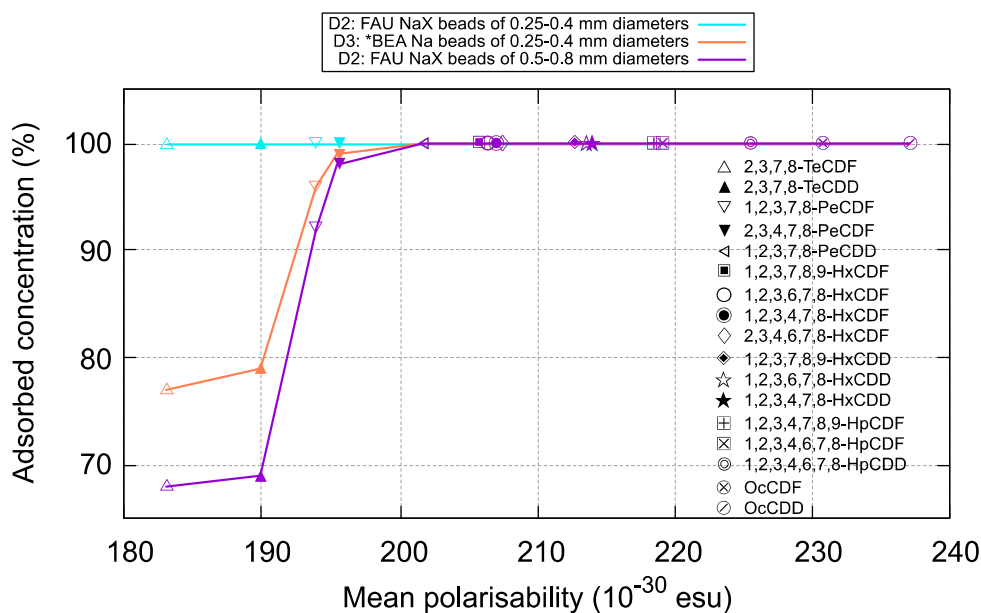
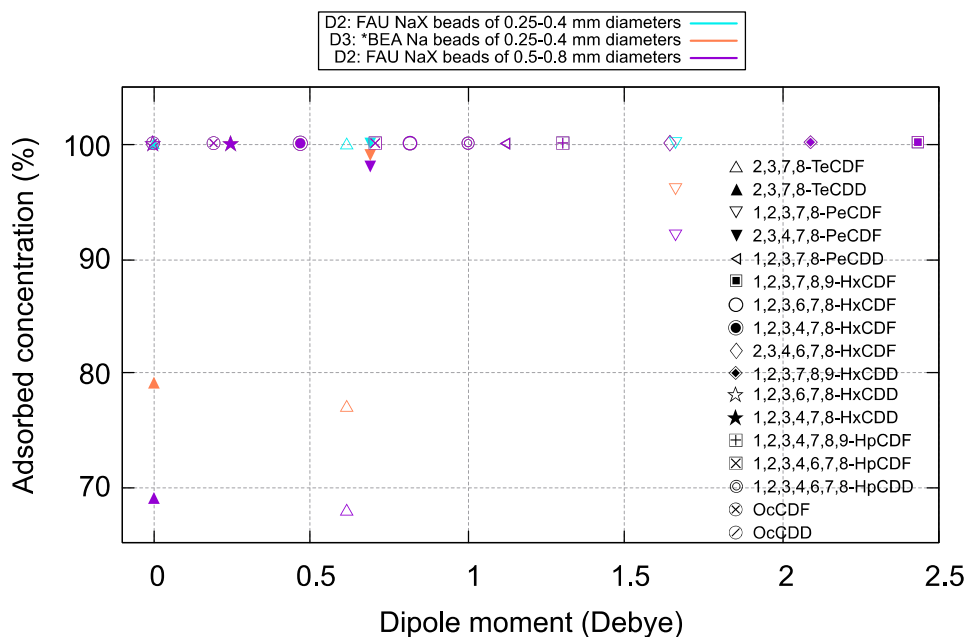
393 In the following results, two different zeolite structure types have been tested in parallel. The  
 394 concentrations of toxic congeners adsorbed onto FAU-NaX and \*BEA-Na beads of 0.25-0.4 mm  
 395 diameters are compared for the sampling D3 in Fig. 7. The breakthrough of 2,3,7,8-TeCDD/F,  
 396 1,2,3,7,8-PeCDF and 2,3,4,7,8-PeCDF has occurred with the \*BEA-Na beads. The same congener  
 397 quantities are measured in the two gas lines, when the quantities of the first and second cartridges are  
 398 added.



399  
 400  
 401 Fig. 7: Concentrations of toxic PCDD/F adsorbed the sampling day D3 in cartridges packed with  
 402 FAU-NaX beads of 0.25-0.4 mm diameters and XAD-2, respectively (top figures, line no. 1) and in  
 403 cartridges packed with \*BEA-Na beads of 0.25-0.4 mm diameters and XAD-2, respectively (bottom  
 404 figures, line no. 2).

405 The relative concentration (%) adsorbed onto an adsorbent is relative to the total concentration  
 406 measured in the gas line. For instance, the relative concentration adsorbed in the first cartridge of the  
 407 line no. 1 is expressed by:  $C_{G11}(c) (\%) = 100 * \frac{C_{G11}(c)}{C_{G11}(c)+C_{G12}(c)}$ . In Fig. 8, the relative concentrations  
 408 of the toxic PCDD/F adsorbed onto FAU-NaX and \*BEA-Na beads of 0.25-0.4 mm diameters, and  
 409 FAU-NaX beads of 0.5-0.8 mm diameters are compared as a function of the dipole moment and

410 polarizability of the congener. A relative adsorbed concentration different from 100 % indicates a  
 411 breakthrough of the congener.



414 Fig. 8: Relative concentration of toxic PCDD/F adsorbed on different zeolites as a function of dipole  
 415 moment (top graph) and of mean polarizability (bottom graph).

416 The breakthrough occurs only for the toxic TeCDD/F and PeCDF with the \*BEA-Na beads of  
 417 0.25-0.4 mm diameters and FAU-NaX beads of 0.5-0.8 mm diameters. There are no correlations  
 418 between the breakthrough (or quantities adsorbed) and the value of the dipole moment of the

419 congeners (top graph of Fig. 8), while the breakthrough increases when the value of the polarizability  
420 diminishes (bottom graph of Fig. 8).

421 None of the toxic PCDD/F can be adsorbed by the micropores of the \*BEA-Na zeolite. So, the  
422 breakthrough observed with \*BEA-Na beads of 0.25-0.4 mm diameters describes the interactions  
423 between the congeners and the external surface area of the \*BEA-Na zeolite. As the beads have same  
424 diameters and external surface area of the \*BEA-Na is larger than that of FAU-NaX, it is expected  
425 that a breakthrough occurs also with the FAU-NaX. However, all the toxic PCDD/F congeners have  
426 been adsorbed by the FAU-NaX beads having the same diameter range than the \*BEA-Na beads. In  
427 addition, those that have been adsorbed by the FAU-NaX and not by the \*BEA-Na can enter the  
428 micropore of the FAU-NaX, only. Therefore, this proves that toxic TeCDD/F and PeCDD/F have been  
429 adsorbed into the micropores of FAU-NaX zeolite.

430 The FAU-NaX beads of 0.25-0.4 mm diameters have an external surface twice larger than the  
431 beads of 0.5-0.8 mm diameters. As a consequence, it could be assumed that a large amount of 2,3,7,8-  
432 TeCDD/F have been adsorbed by the FAU-NaX beads of 0.25-0.4 mm diameters. Furthermore, the  
433 micropore accessibility is twice higher with the smallest beads. Considering this, it can be also  
434 assumed that a part of 2,3,7,8-TeCDD/F measured in breakthrough of the FAU-NaX beads of 0.5-0.8  
435 mm diameters have been adsorbed into the micropores and/or at the entrance of the micropores of the  
436 FAU-NaX beads of 0.25-0.4 mm diameters.

#### 437 **4 Conclusions**

438 If keeping the process parameters (condenser temperatures and gas flows) at the same values, a  
439 constant and reproducible distribution of congeners between the condensate and gas phases can be  
440 insured. Doing that, the total emitted concentrations of toxic congeners can be calculated from only  
441 the concentrations measured in the adsorbent. If a set of adsorbents placed in parallel is required in the  
442 forthcoming monitoring device, the adsorption temperature must be set to a same value in each  
443 adsorbent to ensure same concentrations passing through the adsorbents.

444 In addition, the temperature of adsorption plays an important role to favour specific micropore  
445 adsorption. In the laboratory, a device generating gas stream with synthetic air, moisture vapour,  
446 PCDD/F and solvents in adjustable concentrations is being mounted. This gas stream generator will  
447 supply an EN1948-1 sampling device. By means of this device coupling, the optimal set of values of  
448 the sampling parameters must be estimated in order to specifically adsorb onto zeolites the greatest  
449 and stable amounts of targeted PCDD/F congeners.

450 These very-promising first results prove that FAU-NaX type zeolites can be operated as  
451 adsorbent for sampling the incinerator gas flow. They show the specific adsorption of the toxic  
452 TeCDD/F and PeCDD/F congeners in the micropores of FAU-NaX despite the presence of significant  
453 amounts of moisture and other large amounts of incineration compounds. In a next field campaign,  
454 Faujasite X type zeolites modified by cation exchanges [27,28] will be used in order to adsorb in the  
455 micropore volume larger-size congeners up to OcCDD/F.

## 456 **Acknowledgements**

457 This work has been supported through financial grant of the French Agency for Environment and  
458 Energy Management (ADEME), CORTEA funding program, Project METERDIOX-TER no.  
459 1881C0003.

460 The authors would like to express their sincere thanks to the staff of the waste-to-energy plant of  
461 SUEZ Group.

462 The authors dedicate this paper to the memory of their colleague and friend Oliver SCHÄF died  
463 on Thursday March 19<sup>th</sup>, 2020 after a long illness. For many years, Oliver was invested heavily in this  
464 work.

## 465 **References**

466 [1] F.W. Kutz, D.G. Barnes, D.P. Bottimore, H. Greim, E.W. Bretthauer, The international  
467 toxicity equivalency factor (I-TEF) method of risk assessment for complex mixtures of dioxins and



468 related compounds, *Chemosphere*. 20 (1990) 751–757. [https://doi.org/10.1016/0045-6535\(90\)90178-](https://doi.org/10.1016/0045-6535(90)90178-)  
469 V.

470 [2] M. Van den Berg, L.S. Birnbaum, M. Denison, M. De Vito, W. Farland, M. Feeley, H.  
471 Fiedler, H. Hakansson, A. Hanberg, L. Haws, M. Rose, S. Safe, D. Schrenk, C. Tohyama, A.  
472 Tritscher, J. Tuomisto, M. Tysklind, N. Walker, R.E. Peterson, The 2005 World Health Organization  
473 Reevaluation of Human and Mammalian Toxic Equivalency Factors for Dioxins and Dioxin-Like  
474 Compounds, *Toxicological Sciences*. 93 (2006) 223–241. <https://doi.org/10.1093/toxsci/kfl055>.

475 [3] Directive 2010/75/EU of the European Parliament and of the Council of 24 November 2010  
476 on industrial emissions (integrated pollution prevention and control), European Union Law, 2010.

477 [4] CEN, EN 1948-1: Stationary source emissions - Determination of the mass concentration of  
478 PCDDs/PCDFs and dioxin-like PCBs - Part 1: Sampling of PCDDs/PCDFs, (2006).

479 [5] CEN, EN 1948-2: Stationary source emissions - Determination of the mass concentration of  
480 PCDDs/PCDFs and dioxin-like PCBs - Part 2: Extraction and clean-up of PCDDs/PCDFs, (2006).

481 [6] CEN, EN 1948-3: Stationary source emissions - Determination of the mass concentration of  
482 PCDDs/PCDFs and dioxin-like PCBs - Part 3: Identification and quantification of PCDDs/PCDFs,  
483 (2006).

484 [7] Arrêté du 3 août 2010 modifiant l'arrêté du 20 septembre 2002 relatif aux installations  
485 d'incinération et de co-incinération de déchets non dangereux et aux installations incinérant des  
486 déchets d'activités de soins à risques infectieux, *Journal Officiel de la République Française*, 2010.

487 [8] J. Mayer, H. Linnemann, E. Becker, W. Rentschler, W. Jockel, P. Wilbring, B. Gerchel,  
488 Certification of a long-term sampling system for PCDFs and PCDDs in the flue gas from industrial  
489 facilities, *Chemosphere*. 40 (2000) 1025–1027. [http://dx.doi.org/10.1016/S0045-6535\(99\)00349-5](http://dx.doi.org/10.1016/S0045-6535(99)00349-5).

490 [9] W. Tirlir, G. Voto, M. Donegà, K. Mair, M. Carole, A. Zappi, Validation of a long term  
491 sampling system for PCDD/F, *Organohalogen Compounds*. 73 (2011) 2180–2182.

492 [10] M. Vicaretti, S. Mosca, E. Guerriero, M. Rotatori, Long-term automated sampling of  
493 PCDD/PCDF flue gas: current status and critical issues, *Environmental Science and Pollution*

494 Research. 19 (2012) 1896–1907. <https://doi.org/10.1007/s11356-012-0942-9>.

495 [11] CEN, CEN/TS 1948-5; Stationary source emissions - Determination of the mass  
496 concentration of PCDDs/PCDFs and dioxin-like PCBs - Part 5: Long-term sampling of  
497 PCDDs/PCDFs and PCBs, (2015).

498 [12] R.T. Yang, Adsorbents: Fundamentals and Applications, John Wiley & Sons, Inc., Hoboken,  
499 New Jersey, 2003.

500 [13] C. Baerlocher, L.B. McCusker, D.H. Olson, Atlas of Zeolite Framework Types, sixth,  
501 Elsevier Science, Amsterdam, 2007.

502 [14] J. Patarin, O. Spalla, F. Di Renzo, Inverse Systems - Nanoporous Solids, in: M. Lahami, C.  
503 Bréchnignac, P. Houdy (Eds.), Nanomaterials and Nanochemistry, Springer-Verlag, Berlin Heidelberg,  
504 2007: pp. 305–314.

505 [15] H.J. Fell, M. Tuzcek, Removal of dioxins and furans from flue gases by non-flammable  
506 adsorbents in a fixed bed, Chemosphere. 37 (1998) 2327–2334. [http://dx.doi.org/10.1016/S0045-](http://dx.doi.org/10.1016/S0045-6535(98)00291-4)  
507 [6535\(98\)00291-4](http://dx.doi.org/10.1016/S0045-6535(98)00291-4).

508 [16] P.S. Kulkarni, J.G. Crespo, C.A.M. Afonso, Dioxins sources and current remediation  
509 technologies - A review, Environment International. 34 (2008) 139–153.  
510 <http://dx.doi.org/10.1016/j.envint.2007.07.009>.

511 [17] P. Neumann, K.G. Schmidt, Dioxin separation with natural zeolites, Organohalogen  
512 Compounds. 40 (1999) 543–546.

513 [18] M. Yamashita, T. Wakimoto, H. Nakamura, N. Hamada, K. Honda, Study on the Removal of  
514 Dioxins in Exhaust Gas of Incinerator by Artificial Zeolite, Journal of Environmental Chemistry. 10  
515 (2000) 533–539. <https://doi.org/10.5985/jec.10.533>.

516 [19] R. Jäger, A.M. Schneider, P. Behrens, B. Henkelmann, K.W. Schramm, D. Lenoir, Selective  
517 Adsorption of Polychlorinated Dibenzo-p-dioxins and Dibenzofurans by the Zeolites UTD-1, SSZ-24,  
518 and ITQ-4, Chemistry - A European Journal. 10 (2004) 247–256.

519 [20] B.F. Rordorf, Prediction of vapor pressures, boiling points and enthalpies of fusion for

520 twenty-nine halogenated dibenzo-p-dioxins and fifty-five dibenzofurans by a vapor pressure  
521 correlation method, *Chemosphere*. 18 (1989) 783–788. [http://dx.doi.org/10.1016/0045-](http://dx.doi.org/10.1016/0045-6535(89)90196-3)  
522 6535(89)90196-3.

523 [21] X.-W. Li, E. Shibata, T. Nakamura, Thermodynamic prediction of vapor pressures for  
524 polychlorinated dibenzo-p-dioxins, polychlorinated dibenzofurans, and polybrominated dibenzo-p-  
525 dioxins, *Environmental Toxicology and Chemistry*. 24 (2005) 2167–2177. [https://doi.org/10.1897/04-](https://doi.org/10.1897/04-528R.1)  
526 528R.1.

527 [22] R.T. Yang, R.Q. Long, J. Padin, A. Takahashi, T. Takahashi, Adsorbents for Dioxins: A  
528 New Technique for Sorbent Screening for Low-Volatile Organics, *Industrial & Engineering*  
529 *Chemistry Research*. 38 (1999) 2726–2731. <https://doi.org/10.1021/ie990170o>.

530 [23] H. Xi, Z. Li, H. Zhang, X. Li, X. Hu, Estimation of activation energy for desorption of low-  
531 volatility dioxins on zeolites by TPD technique, *Separation and Purification Technology*. 31 (2003)  
532 41–45.

533 [24] Y. Guan, Y. Liu, W. Wu, K. Sun, Y. Li, P. Ying, Z. Feng, C. Li, Dibenzodioxin Adsorption  
534 on Inorganic Materials, *Langmuir*. 21 (2005) 3877–3880. <https://doi.org/10.1021/la0468545>.

535 [25] M. Mercury, R. Denoyel, A. Simon-Masseron, M. Carette, Y. Zerega, J. Patarin, M. Soulard,  
536 C. Reynard, A. Janulyte, Selective adsorption of 2,3-DCDD and 1,2,3,4-TCDD on \*BEA, EMT, FAU  
537 and MFI-type zeolites as alternative adsorbents for on-line dioxin monitoring, *Adsorption-Journal of*  
538 *the International Adsorption Society*. 17 (2011) 747–758. <https://doi.org/10.1007/s10450-011-9349-z>.

539 [26] M. Mercury, N. Zouaoui, A. Simon-Masseron, Y. Zerega, C. Reynard-Carette, R. Denoyel,  
540 M. Carette, M. Soulard, A. Janulyte, J. Patarin, Adsorption of 2,3-DCDD on FAU and EMT-type  
541 zeolites: Influence of the nature and the content of charge compensating cations, *Microporous and*  
542 *Mesoporous Materials*. 177 (2013) 25–31. <https://doi.org/10.1016/j.micromeso.2013.02.051>.

543 [27] M. Ben Abda, O. Schäf, Y. Zerega, Ion Exchange Effect on Asymmetric Dioxins Adsorption  
544 onto FAU-type X-Zeolite, *Microporous and Mesoporous Materials*. 217 (2015) 178–183.

545 [28] M. Ben Abda, O. Schäf, F. Ziarelli, H. Pizzala, R. Denoyel, S. Viel, Y. Zerega, Investigating

546 the interaction of two asymmetric dioxins with FAU 13X zeolites using calorimetry and solid-state  
547 NMR, *Microporous and Mesoporous Materials*. 234 (2016) 200–206.  
548 <http://dx.doi.org/10.1016/j.micromeso.2016.07.021>.

549 [29] J.D. McKinney, K.E. Gottschalk, L. Pedersen, The polarizability of planar aromatic systems.  
550 An application to Polychlorinated Biphenyls (PCB's), Dioxins and Polyaromatic Hydrocarbons,  
551 *Journal of Molecular Structure*. 105 (1983) 427–438.

552 [30] B.J. Mhin, J.E. Lee, W. Choi, Understanding the Congener-Specific Toxicity in  
553 Polychlorinated Dibenzo-p-dioxins: Chlorination Pattern and Molecular Quadrupole Moment, *Journal*  
554 *of the American Chemical Society*. 124 (2002) 144–148. <https://doi.org/10.1021/ja016913q>.

555 [31] R.S. Asatryan, N.S. Mailyan, L. Khachatryan, B. Dellinger, Electronic elasticity–toxicity  
556 relationships for polychlorinated dibenzo-p-dioxin congeners, *Chemosphere*. 48 (2002) 227–236.  
557 [http://dx.doi.org/10.1016/S0045-6535\(02\)00065-6](http://dx.doi.org/10.1016/S0045-6535(02)00065-6).

558 [32] C. Gu, X. Jiang, X. Ju, G. Yu, Y. Bian, QSARs for the toxicity of polychlorinated  
559 dibenzofurans through DFT-calculated descriptors of polarizabilities, hyperpolarizabilities and hyper-  
560 order electric moments, *Chemosphere*. 67 (2007) 1325–1334.  
561 <http://dx.doi.org/10.1016/j.chemosphere.2006.10.057>.

562 [33] S. Hirokawa, T. Imasaka, T. Imasaka, Chlorine Substitution Pattern, Molecular Electronic  
563 Properties, and the Nature of the Ligand-Receptor Interaction: Quantitative Property-Activity  
564 Relationships of Polychlorinated Dibenzofurans, *Chemical Research in Toxicology*. 18 (2005) 232–  
565 238. <https://doi.org/10.1021/tx049874f>.

566 [34] Y.-Y. Zhao, F.-M. Tao, E.Y. Zeng, Theoretical study of the quantitative structure–activity  
567 relationships for the toxicity of dibenzo-p-dioxins, *Chemosphere*. 73 (2008) 86–91.  
568 <http://dx.doi.org/10.1016/j.chemosphere.2008.05.018>.

569 [35] P.O. Bedolla, G. Feldbauer, M. Wolloch, S.J. Eder, N. Dörr, P. Mohn, J. Redinger, A.  
570 Vernes, Effects of van der Waals Interactions in the Adsorption of Isooctane and Ethanol on Fe(100)  
571 Surfaces, *The Journal of Physical Chemistry. C, Nanomaterials and Interfaces*. 118 (2014) 17608–

572 17615. <https://doi.org/10.1021/jp503829c>.

573 [36] F. Zhang, H.-J. Zhang, J.-P. Chen, X.-M. Liang, Thermal desorption behavior of PCDD/Fs  
574 on the fly ash, *Environmental Science*. 29 (2008) 525–528.

575 [37] G. Rioland, L. Bullo, T.J. Daou, A. Simon-Masseron, G. Chaplais, D. Faye, E. Fiani, J.  
576 Patarin, Elaboration of FAU-type zeolite beads with good mechanical performances for molecular  
577 decontamination, *RSC Advances*. 6 (2016) 2470–2478. <https://doi.org/10.1039/C5RA23258A>.

578 [38] K. Everaert, J. Baeyens, J. Degève, Removal of PCDD/F from Incinerator Flue Gases by  
579 Entrained-Phase Adsorption, *Journal of the Air & Waste Management Association*. 52 (2002) 1378–  
580 1388.

581 [39] J.D. Wilcox, Isokinetic Flow and Sampling, *Journal of the Air Pollution Control*  
582 *Association*. 5 (1956) 226–245.

583 [40] K. Worrall, A. Newton, R. Rao, The analysis of dioxins and furans using HRGC-HRMS  
584 with the AUTOSPEC-ULTIMA NT (Application Note), Waters Corporation, Manchester, UK, 2007.

585 [41] NIST, WebBook of Chemistry, <https://webbook.nist.gov/chemistry/> (accessed May 7,  
586 2020).

587 [42] G. Yang, X. Zhang, Z. Wang, H. Liu, X. Ju, Estimation of the aqueous solubility (K<sub>lgSw</sub>) of  
588 all polychlorinated dibenzo-furans (PCDF) and polychlorinated dibenzo-p-dioxins (PCDD) congeners  
589 by density functional theory, *Journal of Molecular Structure: THEOCHEM*. 766 (2006) 25–33.

590 [43] C. Gu, X. Jiang, X. Ju, X. Gong, F. Wang, Y. Bian, C. Sun, QSARs for congener-specific  
591 toxicity of polyhalogenated dibenzo-p-dioxins with DFT and WHIM theory, *Ecotoxicology and*  
592 *Environmental Safety*. 72 (2009) 60–70. <https://doi.org/10.1016/j.ecoenv.2008.04.003>.

593 [44] M. Tong, D. Zhang, W. Fan, J. Xu, L. Zhu, W. Guo, W. Yan, J. Yu, S. Qiu, J. Wang, F.  
594 Deng, R. Xu, Synthesis of chiral polymorph A-enriched zeolite Beta with an extremely concentrated  
595 fluoride route, *Scientific Reports*. 5 (2015) 11521. <https://doi.org/10.1038/srep11521>.

596 [45] Z. Qin, K.A. Cychosz, G. Melinte, H. El Siblani, J.-P. Gilson, M. Thommes, C. Fernandez,  
597 S. Mintova, O. Ersen, V. Valtchev, Opening the Cages of Faujasite-Type Zeolite, *J. Am. Chem. Soc.*

598 139 (2017) 17273–17276. <https://doi.org/10.1021/jacs.7b10316>.

599 [46] Database of Zeolite Structures, Structure Commission of the International Zeolite  
600 Association. (n.d.). <http://www.iza-structure.org/databases/> (accessed May 28, 2020).

601 [47] L. Whitmore, B. Slater, C.R.A. Catlow, Adsorption of benzene at the hydroxylated (111)  
602 external surface of faujasite, *Phys. Chem. Chem. Phys.* 2 (2000) 5354–5356.  
603 <https://doi.org/10.1039/B008080M>.

604 [48] J. Rouquerol, D. Avnir, C.W. Fairbridge, D.H. Everett, J.M. Haynes, N. Pernicone, J.D.F.  
605 Ramsay, K.S.W. Sing, K.K. Unger, Recommendations for the characterization of porous solids  
606 (Technical Report), *Pure and Applied Chemistry*. 66 (1994) 1739–1758.

607